In Situ Polymerizations of Thiophene on TiO$_2$ Films Using the Semiconductors as Initiators

Zongzhao Wei, Cheng Zou, Xiuyuan Ni

State Key Laboratory of Molecular Engineering of Polymer, Department of Macromolecular Science, Fudan University, Shanghai 200433, China
Correspondence to: X. Ni (E-mail: xyni@fudan.edu.cn)

ABSTRACT: In this work, we prepare the TiO$_2$ nanoparticle film and anatase TiO$_2$ nanoarray film, and we achieve the polymerizations of thiophene using the photoexcited TiO$_2$ film as the initiators. It is measured that the *in situ* polymerizations of thiophene take place on the surfaces of the two films. The growth of polythiophene (PTh) on the TiO$_2$ nanoarray is monitored using Fourier-transform Raman spectroscopy. The TiO$_2$ nanoarray is found to strongly interact with the PTh polymers. It is observed using scanning electron microscope that the microspores in the nanoarray are filled by the polymers after the reaction of 3 h, and the nanoarray is fully covered by the polymer layer when the polymerization lasts for 5 h. The PTh–TiO$_2$ nanoarray composite films are measured for the transient photocurrents and photocurrent-voltage characteristics. The dependence of the photocurrents on the reaction time is revealed and discussed. © 2013 Wiley Periodicals, Inc. J. Appl. Polym. Sci. **2014**, *131*, 40187.

INTRODUCTION

Conjugated polymers that have the substantial electrons delocalizing along the polymer backbones exhibit a number of interesting properties with respect to the electrical conductivity, electrochromism, and luminescence.[1–4] The heterojunction composites consisting of the conjugated polymers and inorganic semiconductors have been the subject of great significance due to the useful electron donor–acceptor attributes.[1–4] Thiophene is an important and popular heterocycle monomer to construct conjugated polymers.[1–4] However, polythiophene (PTh) is not molten in nature and has extremely low solubility in solvents. Thus, it is difficult to use the conventional solution techniques such as blending to prepare the composites of PTh and semiconductor nanoparticles. Alternatively, the electrochemical deposition[5] and photoelectrochemically polymerization[6] have been widely used for preparing the composites of PTh and semiconductor nanoparticles. Meanwhile, substituted thiophene polymers with a good solubility have been synthesized purposely by incorporating alkyl, aryl, or alkysulfonyl groups.[7] From those soluble derivatives, a lot of composite materials, for example, the heterojunction of poly(3-hexylthiophene) and TiO$_2$ nanoparticles,[8] have been prepared by the solution techniques including the spin coating. As reported in the literatures, these materials have been extensively explored for the use in the pho-

toconductive devices,[9,10] memory devices,[11] and polymer solar cells, which promise to offer a good choice as the low-cost, photostable solar cell.[8]

A lot of efforts have recently gone into dissolving the interface problem arising from the incompatibility between the conjugated polymers and inorganic semiconductors.[12] The PTh polymer of intrinsic structure usually lacks a group for anchoring the surface of TiO$_2$ nanoparticles. The weak contact of the polymer with nanoparticles is usually not good for the stability and functions of the composite materials.[13] To improve the interfaces in the heterojunction composites, several strategies have been created for building up interactions between the conjugated polymers and the semiconductors.[12] The Heck coupling steps and clicking reactions have succeeded in combining thiophene polymers with inorganic nanoparticles.[12] Incorporating polar groups (e.g., carboxylic acid, sulfonic acid, or amino group) to the thiophene polymers can also bring them into an intimate contact with the nanoparticles.[7,14] Moreover, there have been reports on coating the nanoparticles with bromine-, amine-, and carboxylic acid-terminated thiophene oligomer,[12,15,16] in which the grafted groups serve to combine with the nanoparticles while the outward heterocycle branches on the surface exhibit the affinity to the polymers. In our previous work, we have reported a polymerization of pyrrole that is initiated by the photoexcited TiO$_2$

nanoparticles.[17] It is important that the conjugated polypyrrole is connected to the nanoparticles immediately after the reaction, thus providing a facile method for preparing the composites. Mechanism investigations have correlated the initiation reaction to the surface-mediated redox at the photoexcited nanoparticles.[17]

The aim of this work is to develop a new composite material of the pristine PTh connected to TiO_2 films using the semiconductor as initiator. At first, we perform the polymerization of thiophene using the easy-to-prepare TiO_2 nanoparticle films as initiators. Thus, we acquire the feasible reaction conditions at which PTh can be synthesized on the photoexcited TiO_2 nanoparticle films. It is known that various semiconductor nanoarrays in the form of nanorods or nanotubes have been synthesized by means of anodic oxidation, hydrothermal reaction, and template growth.[18–20] Because the nanoarrays usually take advantage of rapid electron transfer, the hybrid composite films of the nanoarrays and conjugated polymers promise to provide good materials for the use in the ultraviolet photodetectors[18] and solar cells.[19,20] It is worthwhile to mention that if the semiconducting nanoparticles are used as the electron acceptors, the electrons have to diffuse across numerous contacts among the nanoparticles until they arrive at the electrode and thus, leading to a long-length random path. In this work, we further prepare TiO_2 nanoarray films and achieve the *in situ* polymerizations of thiophene on the TiO_2 nanoarray films. A series of composite films which are prepared in different reaction time are measured about the photoresponse. The results are discussed in terms of film morphology.

EXPERIMENTAL

The TiO_2 nanoparticles (P25, Degussa) were dispersed in the aqueous TritonR X-100 solution and milled into slurry. The slurry was spin-coated on the cleaned indium tin oxide (ITO) glass (10 Ω/sheet) at a speed of 2000 rpm, followed by heating at 450°C for 30 min. The TiO_2 nanoarrays were prepared on the ITO substrate by means of template growth.[19] The templates, which were prepared by placing the seed substrates[20] in an aqueous solution consisting of $0.015M$ $Zn(NO_3)_2$ and $0.015M$ hexamethylenetetramine at 95°C for 2 h, were immersed in the aqueous solution consisting of $(NH_4)_2TiF_6$ ($0.075M$) and H_3BO_3 ($0.2M$) at 25°C for 1.5 h. Subsequently, the as-grown TiO_2 nanoarray on ITO was immersed in H_3BO_3 aqueous solution ($0.5M$) for 1.5 h to remove any trace of ZnO, and then calcined at 400°C for 1 h.

The polymerizations were performed using the TiO_2 films under an ultraviolet irradiation to initiate the thiophene monomers. Each of the TiO_2 films was placed upright in a quartz reactor which was equipped with a water jacket that is connected to a circulator of saturated $CuSO_4$ solution. A 100 ml of the mixture consisting of thiophene (1 g) and copper nitrate (0.24 g) in water was added into the reactor. Copper nitrate serves to increase the photocatalysis of TiO_2. Subsequently, the reactor containing the reactant mixture under stirring was exposed to the ultraviolet irradiation from a mercury vapor lamp. It was determined by a radiometry (UV-A, BJNU Photoelectrical) that

the intensity at the reactor position was 13 mW/cm^2 for 365 nm and 0.085 mW/cm^2 for 254 nm. The other reactions were identical to that of our previous work.[21] The polymerizations lasted for different time. The resulting composite films were washed with water and ethanol, dried under vacuum.

The surface morphologies of films were imaged using the atomic force microscope (AFM) at the tapping mode of Nano-Scope IV and the scanning electron microscope (SEM) using a TS 5136MM instrument. Photofluorescence (PL) emission spectra were recorded on a FLS 920 spectrometer, excited at the wavelength of 406 nm. The X-ray diffraction (XRD) pattern was measured using a PANalytical X'Pert PRO (Cu Kα). Fourier-transform Raman spectra were recorded on a LabRam-1B (Dilor) equipped with a He–Ne laser of 632.8 nm. Electrochemical impedance spectroscopy (EIS) was performed using a three-electrode cell connected to a CHI660C electro-chemical workstation (CHI, Shanghai, China). The working electrode is the powders of the composite materials on the glassy carbon electrode. The transient photocurrents (I–t) and photocurrent–voltage (J–V) curves were measured using a CHI660A electrochemical workstation and 350 W xenon lamp as simulated solar light resource. For the measurement of the J–V curves, the composite films were incorporated into the devices as illustrated in Supporting Information.

RESULTS AND DISCUSSION

Figure 1 shows the PL emission spectra measured from the reactant solutions which use the TiO_2 nanoparticle film as the initiators. The strong peak at the wavelength of 470 nm is assigned to the emission of the thiophene monomers.[7,22] Another band at 515 nm is assigned to polythiophene (PTh) with a chain length exceeding 10 repeat-units.[7,22] It is found that the intensity of the band at 515 nm continues to increase
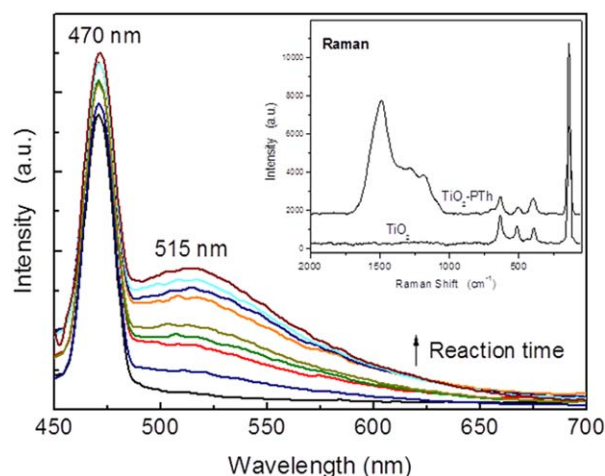

Figure 1. The PL emission spectra of the reaction solutions, measured at different reaction time. The reaction time from the bottom to top is 0, 15 min, 30 min, 45 min, 60 min, 90 min, 120 min, 150 min, and 180 min, respectively. The inset shows the Raman spectra measured for the pristine TiO_2 nanoparticle film and the PTh–TiO_2 composite film, respectively. [Color figure can be viewed in the online issue, which is available at wileyonlinelibrary.com.]

with reaction time, compared to the peak of the thiophene monomers. This result indicates that the polymerization of thiophene takes place. The Raman spectrum of the reacted film is plotted in comparison with the pristine TiO_2 film (the inset to Figure 1). The broad absorption in the wavenumber region from 1000 to 1750 cm^{-1}, which newly appears in the reacted film, is assigned to PTh.[23,24] Thus, PTh is synthesized on the TiO_2 nanoparticle film. Figure 2 shows the AFM photographs imaged from the pristine TiO_2 nanoparticle film and PTh–TiO_2 nanoparticle film, respectively. We can see the shape of the nanoparticles with the sizes from 30 to 40 nm in the pristine TiO_2 film [Figure 2(a)]. As a result of the polymerization, the coarse film is transformed to have a flat surface [Figure 2(b)]. According to the measure by AFM, the root-mean-square roughness (RMS) of the surface decreases from 20 to 10 nm. It is emphasized here that no polymer or oligomer is produced in the control which uses the solution in the absence of TiO_2,[23] as determined by UV–vis spectroscopy. So, the polymerization of thiophene as above is initiated by the photoexcited TiO_2 nanoparticles.

The charge-transfer properties of the TiO_2–PTh composites prepared in different reaction time are investigated using EIS. Figure 3 shows the impedance spectra in the form of Nyquist
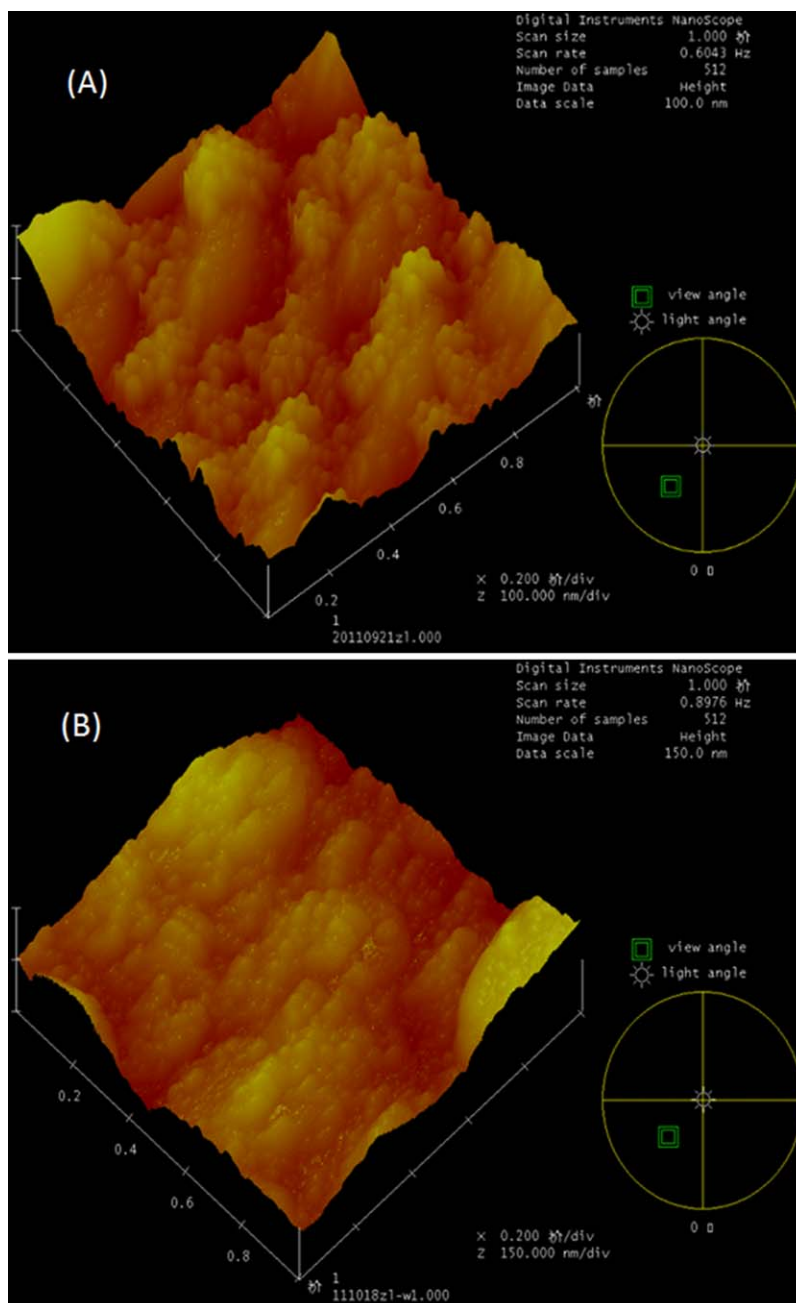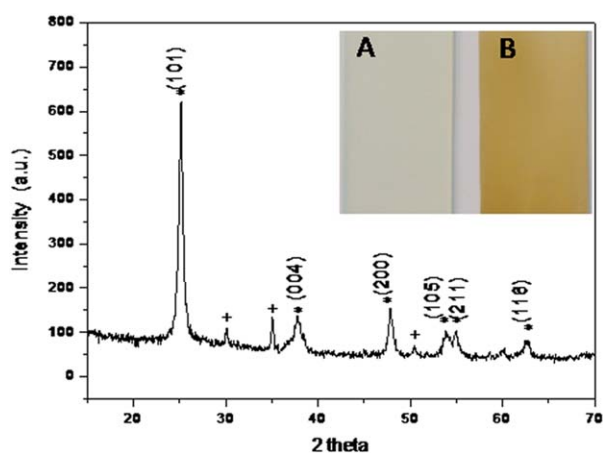

Figure 2. AFM images of (A) TiO_2 nanoparticle film and (B) composite film. [Color figure can be viewed in the online issue, which is available at wileyonlinelibrary.com.]
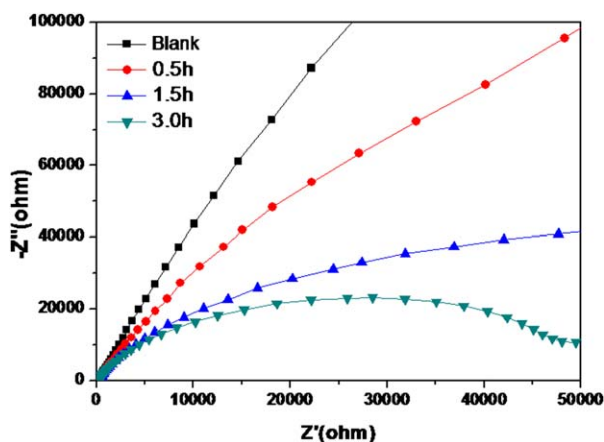
Figure 3. EIS Nyquist plots of electrodes fabricated from the nanoparticle TiO_2–PTh heterojunctions prepared in different polymerization time. [Color figure can be viewed in the online issue, which is available at wileyonlinelibrary.com.]
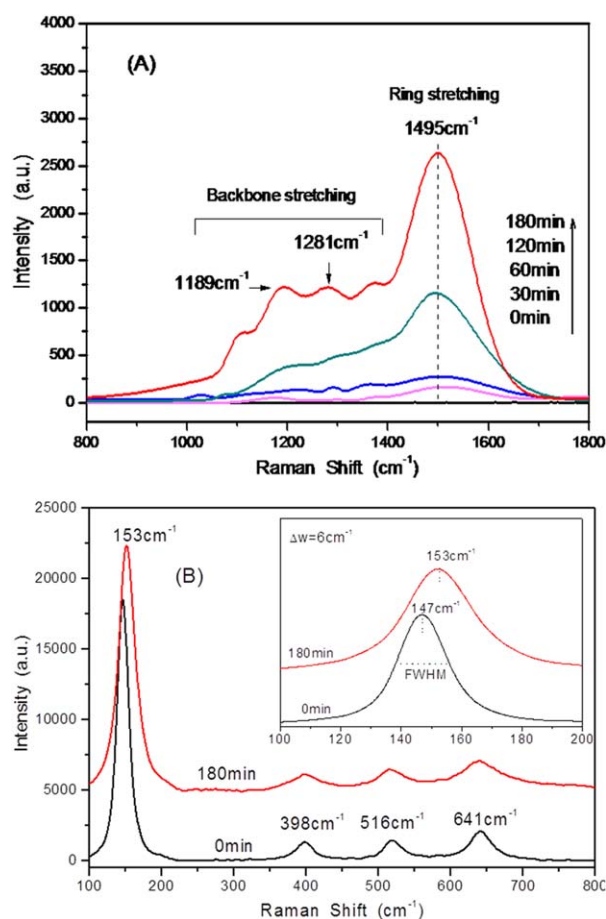
plots (Z'' vs. Z') [25–27] for the TiO_2–PTh composites. It is found that the radii of the arcs are decreased with prolonging the reaction until a complete semicircle takes shape in the testing range. The radius of the arc in a Nyquist plot is proportional to the charge-transfer resistance (R_{ct}) of the testing material.[25–27] So, the TiO_2–PTh composites exhibit lower R_{ct} than the pristine TiO_2, that is, the charge-transfer at the interfaces between the TiO_2 nanoparticles and electrolyte is reinforced by the PTh generation on the TiO_2 surface. To explain the decrease in R_{ct} with increase in reaction time, which is deduced from the EIS curves in Figure 3, we assume that PTh gradually grows on the TiO_2 surface along with the amount of the bare nanoparticles declining continuously.

The synthesized TiO_2 nanoarray film has an average diameter of about 100 nm (see Supporting Information). Figure 4 shows the XRD spectrum of the TiO_2 nanoarray on the ITO substrate. All

diffraction peaks inherent to the planes of anatase TiO_2 are detected in accordance with JCPDS Card No. 84-1286.[20,28] Also in this spectrum, the weak diffraction peaks from ITO are observed, according to JCPDS Card No. 39-1058.[29] This result is attributed to the porous structure in the TiO_2 nanoarray. The macroscopic photograph of the TiO_2 nanoarray film is shown in the inset to Figure 4. As observed, the TiO_2 nanoarray film has a uniform surface. It is measured that the prepared TiO_2 nanoarray here is highly transparent with the transmittance of about 90% (see Supporting Information). It is observed that the nanoarray film turns from transparent into brown after the polymerization, and the color layer is stabilized and resistant to scraping. Figure 5 presents the Raman spectra measured from the reacted films. In the range of long wavenumber [Figure 5(a)], the peak at 1495 cm^{-1} is assigned to stretching of the thiophene rings in PTh. The absorption in the range from 1100 to 1400 cm^{-1} is attributed to the backbone vibration of PTh.[23,24] The split peaks at 1281 cm^{-1} and 1178 cm^{-1} are assigned to symmetric and anti-symmetric stretching of the Cα—Cα' bonds, respectively.[23,24] Each of PTh bands strengthen with the reaction time. Thus, it is concluded that the PTh polymers continue to


Figure 4. The XRD spectrum of the TiO_2 nanoarray on the ITO substrate. The peaks labeled with (*) represent the anatase TiO_2, and the peaks with (+) represent ITO. The inset images are the photographs of (A) the TiO_2 nanoarray and (B) PTh–TiO_2 composite film obtained from the nanoarray TiO_2-initiated polymerization. [Color figure can be viewed in the online issue, which is available at wileyonlinelibrary.com.]

Figure 5. (A) The PTh region of the Raman spectra of the PTh–TiO_2 nanoarray composite film. (B) The TiO_2 region of the Raman spectrum of the PTh–TiO_2 nanoarray composite film prepared after the polymerization of 3 h, in comparison with the neat TiO_2 nanoarray. [Color figure can be viewed in the online issue, which is available at wileyonlinelibrary.com.]

grow on the TiO_2 nanoarray with reaction time. Figure 6 shows the surface morphologies of the PTh–TiO_2 nanoarray composite films and pristine TiO_2 nanoarray film. It is found that the microspores of the nanoarray after the reaction of 3 h are completely filled by PTh along with the nanorod terminals only being seen [Figure 6(b)]. The nanoarray film is fully covered by PTh when the polymerization lasts for 5 h, leading to a dense and uniform surface [Figure 6(c)].

The Raman spectrum of TiO_2 in the TiO_2–PTh composite is compared with that of the pristine TiO_2 nanoarray [Figure 5(b)]. The strongest band of the pristine TiO_2, at 153 cm^{-1}, is assigned

to the E_g mode of anatase TiO_2. The peaks at 398 cm^{-1}, 516 cm^{-1}, and 641 cm^{-1} are assigned to the B_{1g}, A_{1g}, and E_g modes of anatase TiO_2, respectively.[17,30] By comparison, the E_g band of TiO_2 in the composite film is shifted to higher wavenumber by 6 cm^{-1}, and the full-width at half-maximum (FWHM) of the E_g band becomes broader, from 19 to 26 cm^{-1}. Besides the E_g vibration peak, the peaks of the other three modes also show higher FWHM than the pristine TiO_2 [Figure 5(b)]. These results indicate that the TiO_2 nanoarray is interacted with the polymer here. Parker and Siegel have prepared the titanium oxide grains with different O/Ti ratios.[30] They have measured that the E_g band is continuously shifted towards a higher
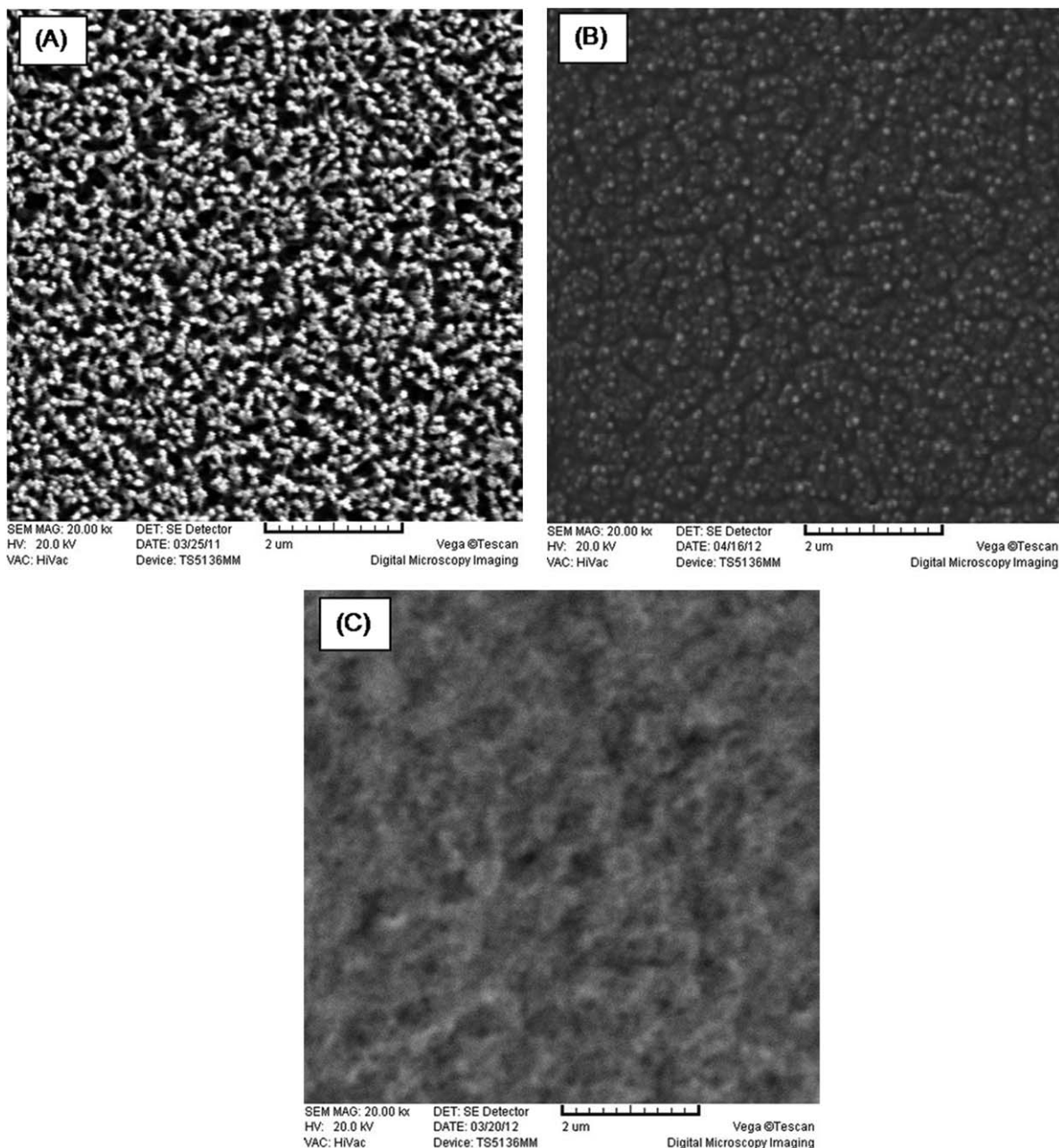
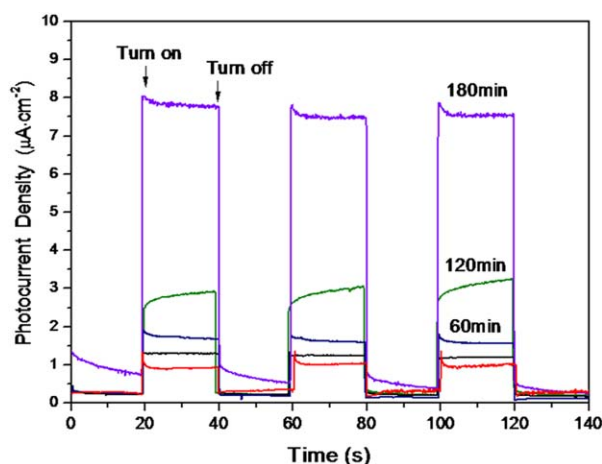
Figure 6. The SEM images (×20,000) of (A) the TiO_2 nanoarray and (B) the PTh–TiO_2 nanoarray composite film obtained from the polymerization of 3 h and (c) the PTh–TiO_2 nanoarray composite film obtained from the polymerization of 5 h.

wavenumber with a decrease in the O/Ti ratio.[30] More recently, similar phenomena that include Raman shifts and broadening have been measured in the modified TiO_2 nanoparticles including N-doped TiO_2.[31] An implication to us is that the PTh polymer here should be linked to the TiO_2 nanoarray. In this case, it is possible for the chemical structure of TiO_2 to be changed.[17,31]

The PTh–TiO_2 nanoarray films, which are prepared in different reaction time, are measured about the transient photocurrents. It is found in Figure 7 that the photocurrent continues to increase until the reaction of 3 h, and the photocurrent is greatly reduced when the polymerization lasts for 5 h. In principles, PTh generates the electron–hole pairs in response to the illumination.[3] According to the energy offset[32,33] as illustrated in the inset to Figure 8, the charge separation takes place at the interface between PTh and TiO_2 nanoarray. The electrons at PTh are injected into TiO_2. Meanwhile, PTh takes a task of transporting holes to Pt electrode.[7] So, the tendency of photocurrents as above can be explained by taking into account the morphologies as shown in Figure 6. The interface between the nanoarray and PTh is extended until the polymerization of 3 h. An increase in the interfacial area may promote the charge separation in this heterojunction.[8] Prolonging the reaction over 3 h should enhance the thickness of polymer layer on the nanoarray, thus leading to longer paths for the holes to diffuse. The polymer layer that is generated from the reaction of 5 h may be too thick for the charges to penetrate across.[3]

Figure 8 shows the J–V curve of the PTh–TiO_2 nanoarray film which is obtained from the polymerization of 3 h. It is obtained that the film has the short-circuit current (J_{sc}) of 0.6 mA/cm², open-circuit voltage (V_{oc}) of 0.39 V, and takes advantage of the good fill-factor (FF)[8,34] as high as 73.2%. It is emphasized here that the heterojunction composites that consist of the conjugated polymers and inorganic semiconductors have been usually used as the photovoltaic materials. The electron–hole pairs, which arise from polymer light-harvesting, are dissociated at the
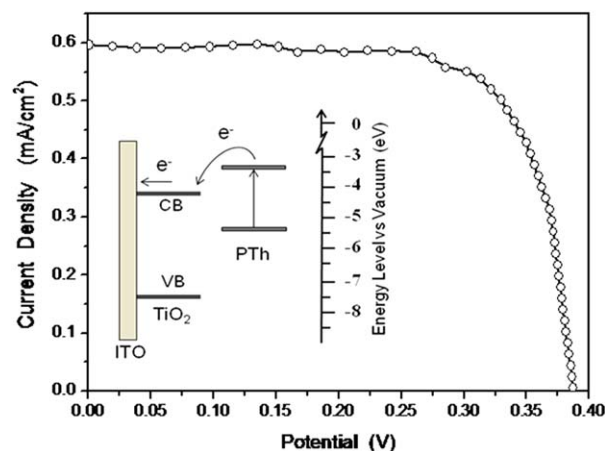
Figure 8. The J–V curve of the device from the PTh–TiO_2 nanoarray composite film obtained from the polymerization of 3 h. The inset shows the energy offset between PTh and TiO_2. CB: conduction band; VB: valence band; LUMO: the lowest unoccupied molecular orbital; HOMO: the highest occupied molecular orbital. [Color figure can be viewed in the online issue, which is available at wileyonlinelibrary.com.]

organic–inorganic interfaces with the electrons injecting into the conduction band of the inorganic semiconductors. The photocurrent is produced once the electron and hole charges are collected by the opposite electrodes, respectively. V_{oc} is usually dominated by the work functions of electrodes which are used in the devices. The V_{oc} value here is comparable to that of other heterojunction devices.[8] It is important that FF is a measure of the ability to transport the charge carriers. The FF as high as 73.2% here approaches the parameter values of the commercial photovoltaic devices and is higher than that of the conventional heterojunction devices in study, which include the nanoarray-based devices.[8,34] The high FF reveals that the charge transfer is facilitated in our composite film.[7,33] This result is attributed to the use of nanoarray and also the organic–inorganic interaction, which is established due to the nanoarray-initiated polymerization here. The interaction promotes the charge dissociation at the interface. Subsequently, the nanoarray provides a direct pathway to transport the electrons to the electrode.

CONCLUSIONS

The anatase TiO_2 nanoarrays were prepared on the ITO substrates. We have achieved the synthesis of polythiophene (PTh) on the nanoarray film using the photoexcited TiO_2 nanoarray to initiate the polymerization. The results from the Raman spectra show that the synthesized PTh is strongly interacted with TiO_2. It is observed that PTh grows on the TiO_2 nanoarray film with the reaction time, along with the microspores in the nanoarray being completely filled after the reaction of 3 h. When the polymerization lasts for 5 h, the nanoarray is fully covered by the PTh layer. This work provides a new method to prepare the composites consisting of PTh and TiO_2 nanoarray. It is found that the photocurrents of the composite films strongly depend on the time of polymerization, and the photocurrents continue to increase until the reaction of 3 h. The composite film can exhibit the photocurrent–voltage curve with

Figure 7. The transient photocurrents of the PTh–TiO_2 nanoarray composite films. The reaction time from the bottom to top is 300 min, 30 min, 60 min, 120 min, and 180 min, respectively. [Color figure can be viewed in the online issue, which is available at wileyonlinelibrary.com.]

a high fill-factor. The EIS spectra have measured lower charge-transfer resistance (R_{ct}) in the TiO_2–PTh composites than the pristine TiO_2.

REFERENCES

1. Heeger, A. J. *Angew. Chem. Int. Ed.* **2001**, *40*, 2591.

2. Quist, P. A. C.; Beek, W. J. E.; Wienk, M. M.; Janssen, R. A. J.; Savenije, T. J.; Siebbeles, L. D. A. *J. Phys. Chem. B* **2006**, *110*, 10315.

3. Chen, J.; Cao, Y. *Acc. Chem. Res.* **2009**, *42*, 1709.

4. Simitzis, J.; Triantou, D.; Soulis, S. *J. Appl. Polym. Sci.* **2010**, *118*, 1494.

5. Fan, B.; Wang, P.; Wang, L.D.; Shi, G.Q. *Sol. Energy Mater. Sol. Cells* **2006**, *90*, 3547.

6. Lee, W.; Roh, S. J.; Hyung, K. H.; Park, J.; Lee, S. H.; Han, S. H. *Solar Energy* **2009**, *83*, 690.

7. Lee, S. J.; Lee, J. M.; Cheong, I. W.; Lee, H.; Kim, J. H. *J. Polym. Sci. Part A: Polym. Chem.* **2008**, *46*, 2097.

8. Brabec, C.; Dyakonov, V.; Scherf, U. Organic Photovoltaics; Wiley-VCH Verlag GmbH& Co. KGaA: Weinheim, **2008**, Chapter 6, pp 179.

9. Zotti, G.; Vercelli, B.; Berlin, A. *Chem. Mater.* **2010**, *22*, 1521.

10. Vercelli, B.; Zotti, G.; Berlin, A. *J. Phys. Chem. C* **2012**, *116*, 2033.

11. Chiu, M. Y.; Chen, C. C.; Sheu, J. T. *Org. Electronics* **2009**, *10*, 769.

12. Zhao, L.; Lin, Z. Q. *Adv. Mater.* **2012**, *24*, 4353.

13. Wang, D. A.; Ye, Q.; Yu. B.; Zhou, F. *J. Mater. Chem.* **2010**, *20*, 6910.

14. Liu, J. S.; Tanaka, T.; Sivula, K.; Alivisatos, A. P.; Frechet, J. M. J. *J. Am. Chem. Soc.* **2004**, *126*, 6550.

15. Jiang, X. X.; Chen, F.; Qiu, W. M.; Yan, Q. X., Nan, Y. X.; Xu, H.; Yang, L. G., Chen, H. Z., *Sol. Energy Mater. Sol. Cells* **2010**, *94*, 2223.

16. Huang, Y. C.; Hsu, J. H.; Liao, Y. C. Chen, W. C.; Li, S. S.; Lin, S. T.; Chen, C. W.; Su, W. F. *J. Mater. Chem.* **2011**, *21*, 4450.

17. Weng, Z.; Ni, X. Y. *J. Appl. Polym. Sci.* **2008**, *110*, 109.

18. Han, Y. G.; Wu, G.; Wang, M., Chen, H. Z., *Appl. Surf. Sci.* **2009**, *256*, 1530.

19. Yu, B. Y.; Tsai, A.; Tsai, S. P.; Wong, K. T.; Yang, Y.; Chu, C. W.; Shyue, J. J. *Nanotechnology* **2008**, *19*, 255202.

20. Yodyingyong, S.; Zhou, X. Y.; Zhang, Q. F.; Triampo, D.; Xi, J. T.; Park, K.; Limketkai, B.; Cao, G. Z. *J. Phys. Chem. C* **2010**, *114*, 21851.

21. Wang, J.; Ni, X. Y. *J. Appl. Polym. Sci.* **2008**, *108*, 3552.

22. Gierschner, J.; Mack, H. G.; Egelhaaf, H. J.; Schweizer, S.; Doser, B.; Oelkrug, D. *Synth. Met.* **2003**, *138*, 311.

23. Yong, Z. Y.; Ni, X. Y. *Langmuir* **2012**, *28*, 4829.

24. Quoc, T. Martin, P.; Niels, H.; Ursula, R.; Waldfried, P.; Jiri, P. *React. Funct. Polym.* **2005**, *65*, 69.

25. Garcia-Belmonte, G.; Boix, P. P.; Bisquert, J.; Sessolo, M., Bolink, H. J. *Sol. Energy Mater. Sol. Cells* **2010**, *94*, 366.

26. Zeng, T. W.; Ho, C. C.; Tu, Y. C.; Tu, G. Y.; Wang, L. Y.; Su, W. F. *Langmuir* **2011**, *27*, 15255.

27. Cihaner, A.; Önal, A. M. *J. Appl. Polym. Sci.* **2008**, *108*, 2373.

28. Wang, J. S.; Cui, Y. T.; Li, H. Y.; Wang, Z. Z.; Huang, K. L.; Sun, G. S. *Res. Chem. Intermed* **2010**, *36*, 17.

29. Han, H.; Mayer, J.; Alford, T. *J. Appl. Phys.* **2006**, *100*, 083715.

30. Parker, J. C.; Siegel, R. W. *Appl. Phys. Lett.* **1990**, *57*, 943.

31. Bacsa, R.; Kiwi, J.; Ohno, T.; Albers, P.; Nadtochenko, V. *J. Phys. Chem. B* **2005**, *109*, 5994.

32. Sanja, T.; Seth, B. D.; Nada, M. D.; Tijana, R.; Steven, J. S. *Small* **2009**, *5*, 1776.

33. Zade, S. S.; Bendikov, M. *Org. Lett.* **2006**, *8*, 5243.

34. Günes, S.; Neugebauer, H.; Sariciftci, N. S. *Chem. Rev.* **2007**, *107*, 1324.